Fringing Electric and Magnetic Field Sensors

Kishore Sundara-Rajan,[1] Alexander V. Mamishev,[1] Markus Zahn[2]

[1]*Department of Electrical Engineering, Sensors, Energy, and Automation Laboratory, University of Washington, Seattle, Washington, USA*
[2]*Department of Electrical Engineering and Computer Science, Laboratory for Electromagnetic and Electronic Systems, Massachusetts Institute of Technology, Cambridge, Massachusetts, USA*

CONTENTS

1. INTRODUCTION

Fringing electric and magnetic field sensors are widely used for non-destructive measurements of material properties. A simple conventional fringing field sensor consists of a sensor head, a current or voltage source, an impedance measurement circuit, and data processing/data acquisition capability. The sensor head is usually a patterned array of electrodes or windings on an electrically insulating substrate. The voltage or current signal is applied to these electrodes and creates, respectively, electric or magnetic fields in the space around the electrodes or windings. These fields penetrate into the materials near the electrodes or windings. Changes of dielectric and magnetic properties of materials affect the distribution of these fields. The impedance measured between the electrical terminals of the sensor head is a function of the material electrical and geometric properties and the electric and magnetic fields. This general principle allows design of sensors for a very broad spectrum of applications including relating changes in electrical properties to physical properties such as temperature, density, defects, moisture, etc.

This chapter provides theoretical background, principles, and examples of design of sensor elements, and description of the most common applications for two types of fringing field sensors, namely, the fringing electric field (FEF) sensors and fringing magnetic field (FMF) sensors. These two types of sensors share many common features and are treated in parallel in the subsequent sections.

2. Theoretical Background

2.1. Maxwell's Equations

All classic electromagnetic phenomena are described by Maxwell's equations. The differential form of Maxwell's equations in linear dielectric and magnetic media is

$$\text{Gauss's Law for } E\text{-Field:} \quad \nabla \cdot (\varepsilon \vec{E}) = \rho \tag{1}$$

$$\text{Gauss's Law for } H\text{-Field:} \quad \nabla \cdot (\mu \vec{H}) = 0 \tag{2}$$

$$\text{Faraday's Law:} \quad \nabla \times \vec{E} = -\frac{\partial}{\partial t}(\mu \vec{H}) \tag{3}$$

$$\text{Ampere's Law:} \quad \nabla \times \vec{H} = \vec{J} + \frac{\partial}{\partial t}(\varepsilon \vec{E}) \tag{4}$$

$$\text{Law of Conservation of Charge:} \quad \nabla \cdot \vec{J} + \frac{\partial \rho}{\partial t} = 0 \tag{5}$$

where $\vec{E}$ is the electric field, $\vec{H}$ is the magnetic field strength, $\vec{J}$ is the current density, ρ is the charge density, μ is the magnetic permeability, ε is the dielectric permittivity, and t is time. The magnetic permeability μ and dielectric permittivity ε can be time and space varying in (1)–(5). Under most sensor application conditions the electromagnetic wave radiation wavelength, $\lambda_{em} = c/f$ where $c = 1/\sqrt{\varepsilon \mu}$ is the speed and f is the frequency of electromagnetic waves, is much longer than sensor periodicity λ of the sensor geometrical structure. For example, a 600 MHz electromagnetic wave has the free-space wavelength of 50 cm. The spatial wavelength of the periodic sensor structures is the distance between the centerlines of the adjacent electrode or winding finger belonging to the same electrode or winding, typically of millimeter order. For quasistatic approximations to be valid, the sensor spatial wavelength has to be much smaller than the radiation wavelength, i.e., $\lambda \ll \lambda_{em}$.

2.2. Electroquasistatics

The operation of fringing electric field sensors is governed by the electroquasistatic approximation to Maxwell's equations. In this approximation, the electric field energy stored in the system is much larger than the magnetic field energy, and the electric field $\vec{E}$ is approximately irrotational ($\nabla \times \vec{E} = 0$). This occurs when the system is capacitive and the time variations are sufficiently slow that the time variation on the right hand side of (3) is neglected. Under the electroquasistatic conditions, Maxwell's equations reduce to:

$$\nabla \cdot (\varepsilon \vec{E}) = \rho \qquad (6)$$

$$\nabla \cdot \vec{J} + \frac{\partial \rho}{\partial t} = 0 \qquad (7)$$

$$\nabla \times \vec{E} = 0 \qquad (8)$$

$$\nabla \times \vec{H} = \vec{J} + \frac{\partial}{\partial t}(\varepsilon \vec{E}) \qquad (9)$$

Figure 1 shows a schematic diagram of a generic model-based fringing electric field sensor. The sensor is comprised of a set of four coplanar electrodes: the driving electrode, the sensing electrode, the guard electrode, and the ground electrode. As the name suggests, the driving electrode is used to excite the sensor. Typically, the driving electrode is connected to an AC voltage source, represented by V_D in Fig. 1. The sensing electrodes are either connected to a voltage measurement circuit or current measurement circuit depending on the detection technique used for the application. When the material under test is present in the near vicinity of the sensor electrodes, the electric fields originating from the driving electrodes penetrate through the bulk of the material under test and then terminate on the sensing electrodes. The dielectric properties of the material under test alter the distribution of the field lines. Hence, the potential or current at the sensing electrodes is also a function of the material's dielectric properties. Thus by studying the variation of sensing current I_S or sensing voltage in the time or frequency domain, material properties can be estimated. To prevent interference from external stray electromagnetic fields, a metal layer in the plane just below the driving and sensing electrodes serves as a ground plane. If there are multiple sensor heads on the same substrate, then guard electrodes are used to prevent "cross-talk" between
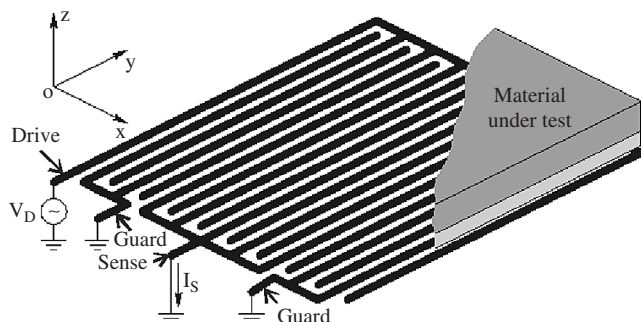
sensors. These electrodes primarily suppress the interaction between adjacent sensor heads. The guard electrodes are either grounded or can be maintained at the same potential as the sensing electrodes.

Electroquasistatic interdigital dielectrometry sensors use spatially periodic electrode structures to generate spatially periodic electric fields that penetrate into adjacent materials under test with dielectric permittivity ε and conductivity σ. The electric field distribution in the Z–X plane of a generic interdigital fringing field sensor in air ($\varepsilon = \varepsilon_0$, $\sigma = 0$) is shown in Fig. 2. The outer driving electrodes in Fig. 2 were excited at 1 V and the center sensing electrode was grounded. The shape of the electric field is independent of frequency while the amplitude depends on the ratio $\omega\varepsilon/\sigma$. Figure 3 shows the variation of the electric field along the normal passing through $x = \lambda/4$. The electric field along the Z axis decays approximately exponentially. Hence, the variations in the permittivity of the media closest to the surface of the electrodes have greater impact on the field distribution than those farther away. The fields die off as $1/r^3$ in the far field as a point electric dipole, where r is the distance between the point dipole and the field position.

Figure 4 shows the electric potential along the same axis as that for Fig. 3. The electric scalar potential obeys Laplace's equation with the electric field penetration depth of the order of $\lambda/2\pi$, where λ is the spatial periodicity of the electrode structure.

Because the electric field has zero curl in (8), $\vec{E} = -\nabla\Phi$ where Φ is the electric scalar potential. When $\rho = 0$ and ε is spatially uniform, (6) reduces to Laplace's equation

$$\nabla^2 \Phi = 0 \qquad (10)$$
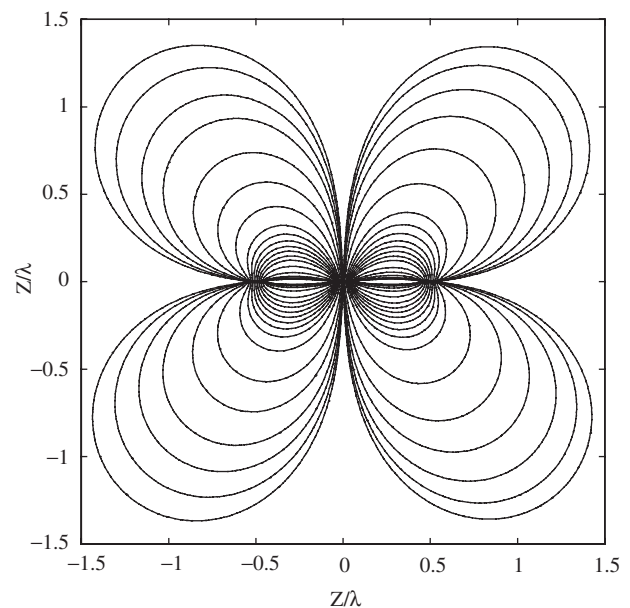
Figure 2. Field distribution of a generic fringing electric field sensor in air. The outer driving electrodes were excited at 1 V and the center sensing electrode was grounded. Each electrode was 0.1λ wide with 0.4λ wide gap between electrodes.

Figure 1. Generic fringing electric field sensor with interdigital pattern of electrodes [1, 2].
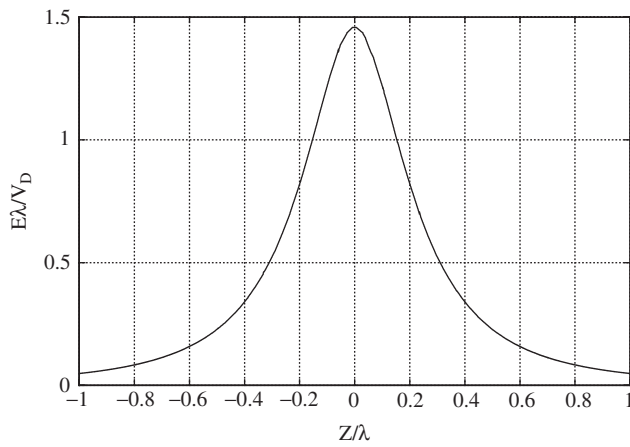
Figure 3. Variation of the non-dimensional magnitude of the electric field as a function of z along the $x = \lambda/4$ line midway between sense and drive electrodes. The drive electrodes were maintained at $V_D = 1$ V and the sense electrode was grounded.

The potential as a function of position for $z > 0$ can be written as a Fourier series

$$\Phi(x, z) = \sum_{n=1}^{\infty} \Phi_n \cos(k_n x) e^{-k_n z} + \Phi_0 \frac{z}{\lambda}, \quad k_n = \frac{2n\pi}{\lambda} \quad (11)$$

The coefficients Φ_0 and Φ_n can be found by evaluating (11) at $z = 0$, where the potentials are constant on each drive and sense electrode, and must be solved by numerical techniques in the space between the electrodes.

2.3. Magnetoquasistatics

The operation of fringing magnetic field sensors is governed by the magnetoquasistatic approximation. In this approximation, the magnetic field energy stored in the system is much larger than the electric field energy, the system is inductive, and the time variations are sufficiently slow that
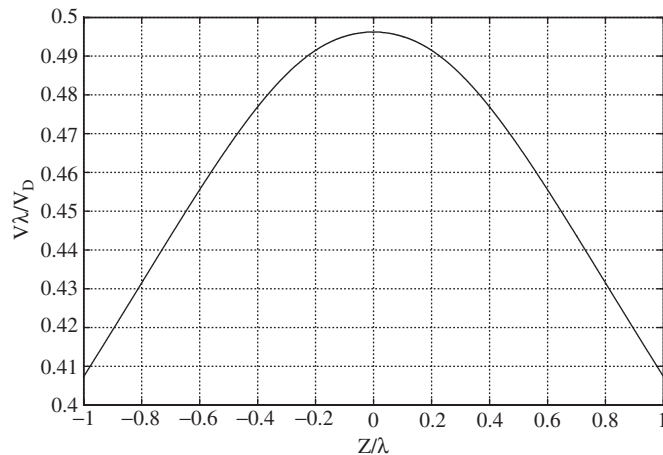
Figure 4. Variation of the non-dimensional potential as a function of z along the $x = \lambda/4$ line midway between sense and drive electrodes. The drive electrodes were maintained at $V_D = 1$ V and the sense electrode was grounded.

the displacement current density on the right side of (4) is negligible. Under magnetoquasistatic conditions, Maxwell's equations reduce to:

$$\nabla \cdot (\varepsilon \vec{E}) = \rho \quad (12)$$

$$\nabla \cdot \vec{J} = 0 \quad (13)$$

$$\nabla \times \vec{E} = -\frac{\partial}{\partial t}(\mu \vec{H}) \quad (14)$$

$$\nabla \times \vec{H} = \vec{J} \quad (15)$$

$$\nabla \cdot \vec{B} = 0 \quad (16)$$

Figure 5 shows a schematic diagram of a generic fringing magnetic field sensor. The sensor consists of two sets of windings, the primary and secondary, generally on a substrate under the material under test. When electric drive current I_D passes through the windings, it induces eddy currents in the conducting material under test. Magnetic permeability of the material also results in an increase of mutual inductance between secondary and primary windings. The open-circuit secondary winding voltage is given by the time-rate change of magnetic flux passing through the secondary winding due to the current in the primary winding.

Quasistatic magnetometry sensors often have spatially periodic windings to generate spatially periodic magnetic fields that penetrate into adjacent materials under test. Because the divergence of $\vec{B}$ in (16) is zero, a magnetic vector potential can be defined as

$$\vec{B} = \mu \vec{H} = \nabla \times \vec{A} \quad (17)$$

For ohmic conducting material, so that $\vec{J} = \sigma \vec{E}$, substituting (17) into (15) with μ and σ held constant yields a diffusion equation for $\vec{A}$

$$\nabla^2 \vec{A} - \mu\sigma \frac{\partial \vec{A}}{\partial t} = 0 \quad (18)$$

where we use the gauge condition $\nabla \cdot \vec{A} = 0$. For the sensor in Fig. 5 in the sinusoidal steady state at radian frequency ω,
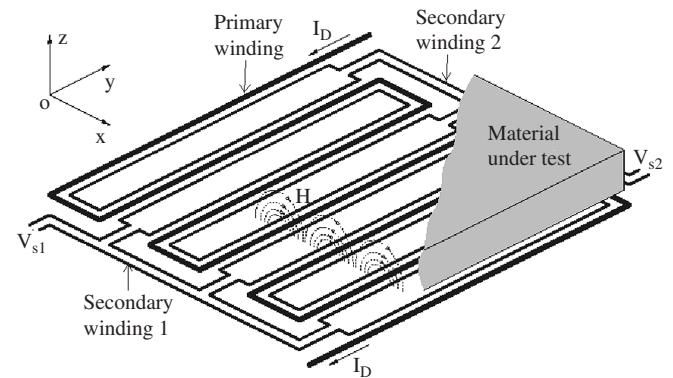
Figure 5. Generic fringing magnetic field sensor with meandering pattern of windings [1–3]. (Reprinted with permission from [1], A. V. Mamishev et al., *Proceedings of the IEEE* 92(5), 808–845 (2004). © 2004, IEEE.)

we neglect variation with the *y* coordinate so that the vector potential is of the form

$$\vec{A} = Re[\hat{A}_y(x, z)e^{i\omega t}] \qquad (19)$$

so that (18) reduces to

$$\nabla^2 \hat{A}_y - i\omega\sigma\mu\hat{A}_y = 0 \qquad (20)$$

where $\hat{A}_y$ is the space varying complex amplitude of A_y.

Then the solution of (20) is the Fourier series

$$\hat{A}_y(x, z) = \sum_{n=1, \text{odd}}^{\infty} A_n \cos(k_n x)e^{-\gamma_n z} \qquad (21)$$

where the complex spatial decay coefficient is

$$\gamma_n = \sqrt{k_n^2 + i\omega\sigma\mu} = \sqrt{k_n^2 + 2i/\delta^2}; \quad k_n = 2\pi n/\lambda \qquad (22)$$

with $\delta = \sqrt{2/(\omega\mu\sigma)}$ known as the skin-depth.

Such sensors are used for measurements of conductivity, complex magnetic permeability, and material thickness for single and multiple layered magnetic and/or conducting media. Typical non-destructive testing and evaluation applications include gas turbine component quality assessment [4]; cold work quality assessment and fatigue characterization [5, 6]; and quality control measurements of aircraft propeller blades [7].

2.4. Spectroscopic Systems

All dielectric and magnetic materials consist of electric or magnetic dipoles. When subjected to an external electric or magnetic field, these dipoles re-align so as to partially neutralize the effect of the external field. This re-alignment of dipoles occurs to a varying extent for different materials. Thus, the dielectric or magnetic response of each material across the frequency spectrum is different, and in most cases, unique. The study of this response variation is known as dielectric or magnetic spectroscopy.

The dielectric or magnetic response of a material is generally quantified in terms of its complex dielectric permittivity or magnetic permeability. The complex dielectric permittivity $\varepsilon^*(\omega)$ or magnetic permeability $\mu^*(\omega)$ is usually represented as,

$$\varepsilon^*(\omega) = \varepsilon'(\omega) - i\varepsilon''(\omega) \qquad (23)$$

$$\mu^*(\omega) = \mu'(\omega) - i\mu''(\omega) \qquad (24)$$

where $\varepsilon'(\omega)$ and $\mu'(\omega)$ are the real parts representing capacitive or inductive energy storage and $\varepsilon''(\omega)$ and $\mu''(\omega)$ are the loss.

For all materials, the loss factor is a function of excitation frequency. The loss factor mechanisms are schematically shown in Fig. 6. For a few low-loss materials and non-polar materials the variation in the loss factor with frequency is predominantly due to distortion in the electron clouds. Hence, the magnitude of variation of loss factor is negligibly small.
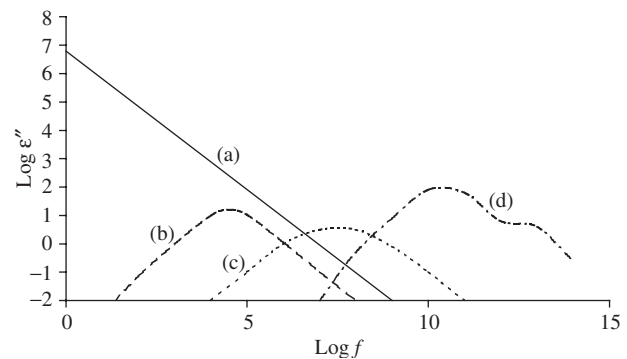
Figure 6. Mechanisms influencing the loss factor of a moist material over a wide range of frequencies f (Hz). (a) DC conductivity, (b) Maxwell–Wagner polarization, (c) dipolar polarization of water bound to the matrix of the material, (d) dipolar polarization of free water [8].

The polarization of molecules arising from their reorientation with the imposed electric field is the most important phenomenon contributing to the loss factor in the radio and microwave frequency ranges (10^7 to 3×10^{10} Hz). This includes the dipolar polarization due to bound and free water relaxation. At infrared and visible light frequencies, the loss mechanisms due to atomic and electronic polarization (collectively known as distortion polarization) are the dominating loss mechanisms [8].

The description for the process for pure polar materials was developed by Debye in 1929 [9]. The Debye dielectric relaxation model is the simplest way to analyze polarization in purely polar materials. The complex dielectric permittivity for the Debye relaxation model with a single relaxation time τ and DC magnetic susceptibility χ_0 is

$$\varepsilon^*(\omega) = \varepsilon_0 \left(1 + \frac{\chi_0}{1 + i\omega\tau}\right) \qquad (25)$$

so that

$$\varepsilon'(\omega) = \varepsilon_0 \left(1 + \frac{\chi_0}{1 + (\omega\tau)^2}\right) \qquad (26)$$

$$\varepsilon''(\omega) = \frac{\varepsilon_0 \chi_0 \omega\tau}{1 + (\omega\tau)^2} \qquad (27)$$

The model assumes that the relaxation process is governed by first order dynamics, and hence can be characterized with a single time constant. The model can be derived using basic laws of polarization and conduction [10]. Magnetic materials have analogous frequency dispersion in the complex magnetic permeability.

3. INSTRUMENTATION

3.1. Architecture

The success of any kind of sensing technique depends heavily on the ability to accurately measure the sensed voltages or currents without influencing them. Though the actual circuit used for measuring the voltages and currents differ with application and personal preferences, the main building blocks remain the same. Figure 7 shows the schematic
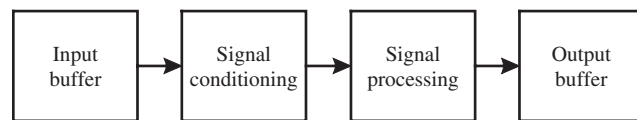
Figure 7. Schematic representation of the constituent blocks of a generic measurement circuit.

representation of the generic measurement circuit used with fringing field sensors. The measurement circuit can be broken down to four circuit blocks: (a) Input Buffer, (b) Signal Conditioning Circuit, (c) Signal Processing Circuit, and (d) Output Buffer.

The most important part of any measurement circuit is the input buffer. In any cascaded system, such as the one shown in Fig. 7, the contribution of the very first stage to the overall noise factor of the system is the highest of all stages. Hence, when designing measurement circuits, a very low noise instrument amplifier with unity gain is usually used as the very first stage. One of the main requirements of the input amplifier is that it does not load the sensor beyond the sensor's driving capability. That is, the input impedance of the buffer has to be very high.

The second stage of the measurement circuit is the signal conditioning stage. Here the signal from the buffer is usually amplified in both power and voltage. The strengthened signal is then conditioned by passing it through a set of filters to remove extraneous frequencies. The most common approach is to cascade a low pass filter set to filter all the frequencies below the frequency of interest, and a high pass filter to filter out any frequency above it. This in effect creates a band-pass filter. The main reason for adopting a two-filter approach rather than a single band pass filter is that it is possible to tune the cutoff frequencies of each of the filters by varying just one circuit component. This is a major advantage in spectroscopic systems, where the frequency of interest is not a constant, and the circuits have to be designed to accommodate a range of frequencies rather than just one frequency.

The third stage of the measurement circuit is the signal processing stage. This stage primarily extracts the information from the measured signals. The most common way to implement this stage is to use a microcontroller or a microprocessor. The exact architecture and the requirements of the signal processing circuit depend on the application requirements.

The fourth and final stage of the circuit is the output buffer stage. The main purpose of the output buffer is to electrically isolate the preceding stages from the rest of the system components. The output buffers are designed to have very high driving capabilities, and are usually designed with high power components. In cases where power is an important issue, the output impedance of the buffer is designed to match the input impedance of the subsequent system blocks.

3.2. Multiple Channel Systems

Multiple sensor heads are used in measurement systems that require data from multiple physical locations on the material under test, or which require data at different penetration depths. The design of the data acquisition system for such

applications is more complicated than that for single sensor heads.

There are two principal approaches to the design of multiple channel systems. One method uses a dedicated measurement system for each of the sensor heads. The other approach is to share a single measurement circuit between multiple sensors using time domain multiplexing (TDM). Figure 8 shows the schematic representation of one such TDM system.

All the sensors are connected to a multiplexer circuit. The output of the multiplexer unit is then connected to a measurement circuit, the output of which is then demultiplexed into individual output channels. The input multiplexer is often a low impedance, non-bounce static relay. The output demultiplexer is a digital switch in the case of digital outputs or is again a static relay in case of analog outputs. The operation of the system is controlled by a master timer.

The multiple dedicated measurement circuit is most useful where simultaneous monitoring of multiple sensors is required. However, the cost of such a system increases proportionally to the number of sensors.

TDM measurement systems are used when the sensors need not be measured at exactly the same instant of time. These systems tend to be much less expensive than the dedicated channel systems. However, TDM systems cannot be used to measure fast varying signals, as the acquisition speeds are limited by the switching speeds of the multiplexer and demultiplexer. It is a good design practice to introduce redundancy in the measurement circuit in the case of TDM systems to improve their reliability.

3.3. Sensing Circuits

Irrespective of the sensor head design, the control architecture, and the associated electronics for evaluating any property of the material under test, one needs to measure the terminal quantities across the electrodes of the sensor, and interpret them as variations in the complex dielectric permittivity or magnetic permeability of the material by use of an equivalent lumped element circuit. The variations in the permittivity and permeability can then be mapped onto the physical material property through calibration-based algorithms. The circuit used to measure the terminal property
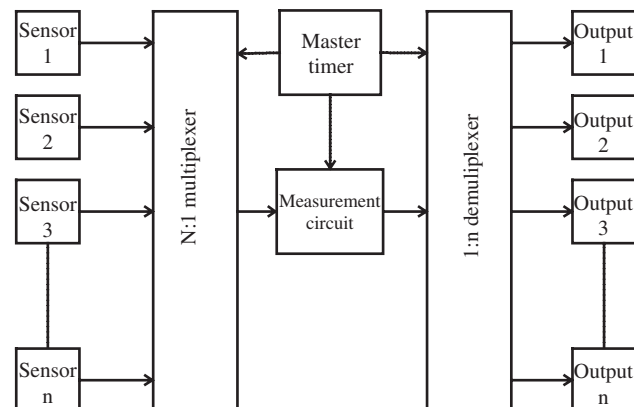
Figure 8. Schematic representation of a multiple sensor data acquisition system.

of the sensor can be broadly classified into two major categories, voltage sensing circuits, and current sensing circuits. The operation of each kind of circuit is explained in detail in the following sections.

3.3.1. Voltage Sensing Circuits

As the name suggests, this family of circuits help determine the variations in the complex dielectric permittivity and magnetic permeability of the material under test by measuring voltages across the sensor electrodes.

A sinusoidal AC voltage, V_D, is applied between the driven electrodes and ground in a fringing electric field sensor. Due to the potential difference, the electric fields originate from the driven electrodes, pass through the bulk of the material under test and terminate at the sensing electrodes. Thus by measuring the voltage across the sensing electrode and ground, V_S, the properties of the material can be deduced. Usually, to prevent ambient electromagnetic fields from interfering in the operation of the sensor, a metal plane below the substrate plane of the sensor electrodes is grounded. Figure 9 shows the schematic of an interdigital fringing electric field sensor connected to a voltage sensing circuit.

One of the disadvantages of this sensing method is that there is a potential difference across the substrate between the sensing electrodes and the ground plane. Hence some charge is lost in the parasitic coupling between the sensing electrodes and the ground. This can be a non-negligible source of error in micro sensors where the current flowing through the circuit is on the order of a few fA. Figure 10 shows the guard plane layout of a voltage sensing circuit that circumvents this problem.

The difference between the setups shown in Fig. 9 and that shown in Fig. 10 is that the back plane in Fig. 9 is grounded while that in Fig. 10 the guard voltage V_g is maintained at the same voltage as the sensing electrodes. Since in the latter case there is no potential difference between sensing electrodes and the back plane there is no drainage of charges through the parasitic coupling between these two electrodes.
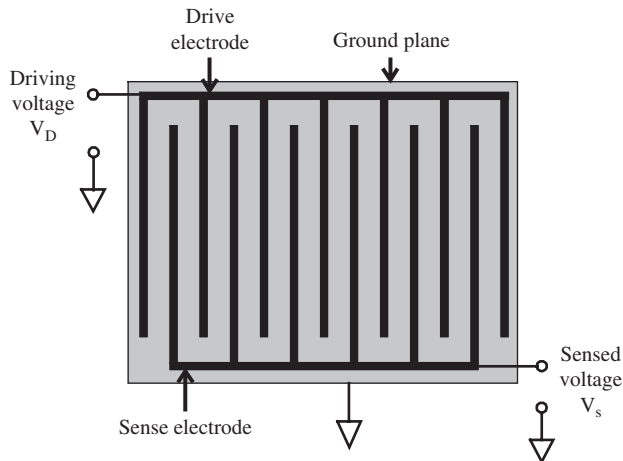
Figure 9. Schematic representation of a fringing electric field sensor connected in voltage sensing configuration with its back plane grounded.
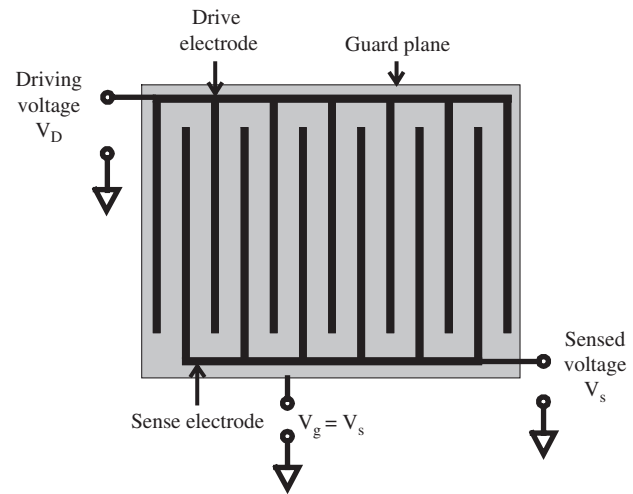
Figure 10. Schematic representation of a fringing electric field sensor connected in voltage sensing configuration with its back plane guarded.

### 3.3.2. Current Sensing Circuits

Current sensing circuits are used for measuring terminal properties of magnetic field sensors and for measuring very high impedances with electric field sensors. This method is very sensitive to very low values of current, and hence is the preferred method for microsensing applications.

A fringing magnetic field sensor, like that in Fig. 5, connected in current sensing mode has the primary or driving winding connected across an AC voltage source. The secondary windings are connected in short circuit configuration, $V_{s1} = V_{s2} = 0$, with an ammeter in series to measure the short circuit current. The current flowing through the primary creates the magnetic field. This magnetic field is coupled to the secondary or sensing windings, thus inducing currents in them. When a magnetic material is present in the vicinity of the sensor, it redistributes the magnetic fields, thus changing the short circuit current.

For an electric field sensor, an AC voltage is applied across the drive and ground electrodes. The electric field lines originate from the driven electrodes, pass through the bulk of the material under test, and terminate on the sensing electrodes, thus raising the sensing electrode charge. The sensing electrodes are virtually grounded, and the short circuit current is measured. The ratio of the input voltage and the measured current is the sensor transimpedance and is a function of the dielectric properties of the material under test. Figure 11 shows the schematic layout of one such current sensing circuit.

3.4. Circuit Design

Ground Most of the voltages measured in a sensing system are with respect to the ground. In a large measurement system, there are often multiple virtual grounds. That is, each section of the system has its own reference potential. It is important to remember that these ground potentials may not always be the same. Hence, there exist small stray capacitances between the virtual grounds. These stray capacitances lead to small leakage currents. These currents have to be considered when designing the measurement system.
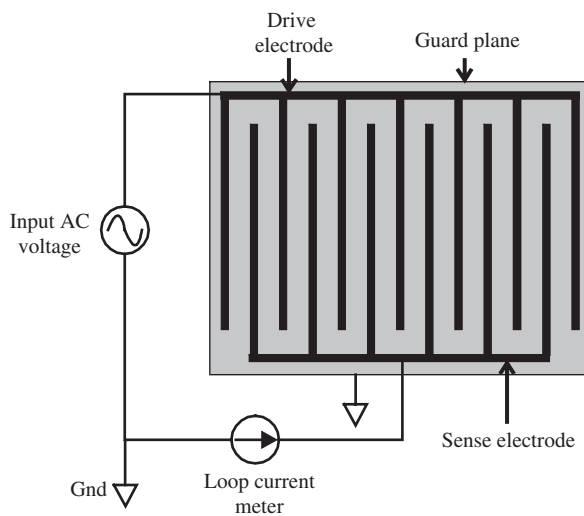
Figure 11. Schematic representation of a fringing electric field sensor configured in current sensing mode.

Most modern measurement systems have digital components, such as analog to digital converters. It is a good design practice to maintain separate virtual grounds for the analog components and the digital components. This prevents the high current/voltage power switching components from interfering with the operation of the digital components, which operate at much smaller voltages.

Data Acquisition The front end of the data acquisition system is nearly always an instrument amplifier. Most of these amplifiers are implemented using operational amplifiers. The operational amplifiers have an inherent frequency limit of operation, beyond which the gain of the amplifier starts to drop. This frequency limit, known as the corner frequency, f_c, varies as a function of the input impedance, and is defined as the frequency at which the amplitude of the output signal drops by 3 dB. For a purely resistive circuit, the output voltage V of the amplifier is related to the input voltage e at a frequency f as:

$$V = \frac{e}{\sqrt{1 + (f/f_c)^2}} \tag{28}$$

It can be noted from (28), that the higher the corner frequency, the higher is the accuracy of the measured voltage. Hence, it is critical to choose the input impedance of the amplifier such that all the frequency components of interest can be measured accurately. Also of importance is the response speed of the amplifiers. Most modern amplifiers can be programmed to operate in different response domains by varying their bias currents. The higher the bias current, the faster is the response of the amplifier. However, this additionally loads the sensor, and hence it is necessary to strike a balance between both.

Detailed discussions on the design of individual components of the electronic circuitry can be found in [11], and that of the general concepts of acquisition system design can be found in [11, 12].

3.5. Advantages of Fringing Field Sensors

3.5.1. One-Side Access

Several inherent advantages of the planar interdigital geometry attract device designers. One of the most important ones, especially for non-destructive testing (NDT) sensors and piezoacoustic transducers, is that only a single-side access to the test material is required. One can penetrate the sample with electric, magnetic, acoustic, or optical fields from one side of the sample, leaving the other side open to the environment, which can allow absorption of gas, moisture, or chemicals that change electrical properties of the material under test (MUT). A sensitive layer of chemical or biological nature deposited over the electrodes and windings can also interact with a gas or liquid environment, allowing monitoring of concentration of chemicals in such materials as air, transformer oil, or the human body. In some situations, the other side of the material sample may be too far away, or inaccessible due to design limitations for an electrode so that one-sided access is essential.

3.5.2. Control of Signal Strength

By changing the area of the sensor, the number of fingers, and the spacing between them, one can control the strength of the output signal. A trade-off between the signal-to-noise ratio and the minimum sensing area is selected based on the application requirements. In microchip sensors, the size of the sensitive area is usually of little consequence, whereas in imaging devices it plays a major role.

3.5.3. Imaging Capability

Either by moving sensor heads or by forming sensor arrays, one can interrogate different regions of material under test. A simple interdigital structure can be moved up and down to measure the depth profile or float above the material surface to measure variation of changes at a specified depth. A combination of both potentially provides a 3D image of the material under test, but simple interdigital sensors are rarely used in this manner because it can take a long time to scan a sample.

4. APPLICATIONS

4.1. Structural Non Destructive Testing

Direct sensing is the easiest and simplest form of sensing. In this method, the change in the property of interest is directly measured by the sensors. The most common use of this sensing technique using electromagnetic sensors is to detect the presence or absence of an object or defect in the field of interest. Any material, crack, void, or inclusion within the field of the EM sensor will distort the electromagnetic field distribution. This distortion can be detected by measuring the changing impedance of electrical or magnetic sensors.

Perhaps the simplest type of electric field sensor is the "Stud finder" [13]. These sensors indicate the position of the studs in a wall without physically penetrating the wall. This sensor has a single set of driving and sensing electrodes. The electrodes are held flat across the surface of the wall, and moved parallel to the floor. In the normal state, i.e.,

when the sensor is held against just the dry wall, the effective dielectric constant as seen by the sensor is a combination of that of the dry wall and air. Since the thickness of dry wall is relatively small, the effective dielectric constant is close to that of air. Hence, the measured capacitance across the electrodes is the least in this position. When the sensor encounters a stud, the effective capacitance as seen by the sensor is a combination of that of the dry wall and the stud, and hence is higher than ambient. By measuring the change in capacitance as the sensor moves along the surface of the wall, the position of the stud can be determined. A very similar application is detection of presence and position of a passenger in the seat of a car to determine if an air bag needs to be deployed, and in the fashion in which it has to be deployed. Here, large electrodes are embedded in the seat, backrest, and the head rest of the car seats. By measuring the capacitance changes in each of the individual sensors, the position of the passenger can be determined [14–16].

A similar application for magnetic sensing is the metal detector [17, 18]. There are two kinds of metal detectors, the very low frequency detectors (VLF) and the pulse induction (PI) detectors. The VLF detectors have two coils, the transmitter coil and the receiver coil. The transmitter coil is attached to a low frequency signal generator. When an AC current flows through the transmitter coil, it generates an electromagnetic field. These time varying field lines change the magnetic flux through the receiver coil, thus changing the voltage across it. This operation is similar to that of an electrical transformer. The effective inductance of the coil depends on the conductivity and the magnetic permeability of the coupling media. When a non-magnetic metal is introduced into the field of the sensor, the effective permeability of the media is decreased because of the induced eddy currents. This lowers the value of the inductance, and hence the voltage across the receiver coil. A magnetic material will raise the inductance. By measuring the change in the voltage across the receiver coil, the presence or absence of a conducting or magnetizable metal can be ascertained. In addition to the change in magnetic permeability, in magnetic metals like iron, there is both a current induced in them, which alters the distribution of the magnetic field, and a magnetization effect. This change in magnetic field distribution changes the flux linkage and thus changes the voltage across the receiver coil.

Figure 12 shows the schematic representation of an eddy current sensor. The sensor consists of two sets of coils, the reference coil and the sensing coil. When a current flows through each of these coils, in the absence of any conductive material in the vicinity, the coils are balanced. When a conductive material is introduced near the coils, the magnetic fields from the sensing coils interact with the bulk of the conductive material and produce eddy currents in the bulk. The eddy currents flow in such a way as to oppose the current flow in the sensing coil. This creates an imbalance between the reference and the sensing coils. By using a bridge circuit, the presence of conductive materials can thus be indicated.

Figure 13 shows the magnetic field distribution in free space in the presence of the conductive material ($\sigma = 3.7e7$, $\mu_r = 1$). The sensing coil and the reference coils each of radius 0.01 m were excited at 100 Hz using individual 1 A

Figure 12. Schematic representation of an eddy current sensor [11].

current sources flowing in the Z direction. The skin depth δ is 8.3 mm. The line $x = 0$ is an axial boundary, i.e., there is an exact mirror image of the coils and the conductive material on the other side of the line $x = 0$. In the absence of the conductive material, the isopotential lines are symmetric about the line $y = -0.03$ (the mid point between the sensing and reference coils). When the conductive material is introduced, the eddy currents distort the field distribution near the sensing coil. This change in field distribution is reflected as change in terminal impedance of the sensing coil.

Another application of eddy sensors is to detect small displacements. When the conductive material is displaced by a small distance, the strength and distribution of magnetic fields that interact with the bulk of the material changes, thus altering the magnitude of the eddy current.
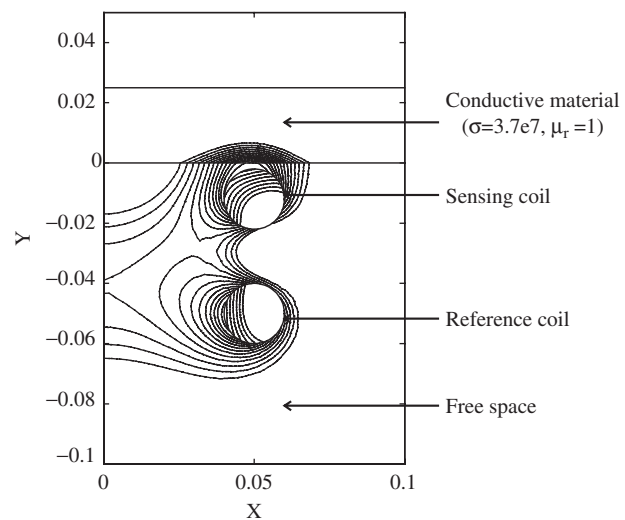
Figure 13. Magnetic field distribution of an eddy current sensor in free space. The sensing coil and the reference coils each of radius 0.01 m were excited at 100 Hz using individu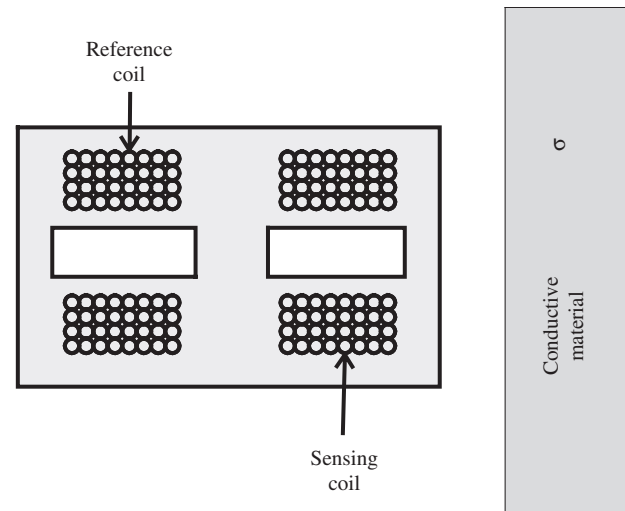al 1 A current sources flowing in the Z direction. The conductive material ($\sigma = 3.7e7$, $\mu_r = 1$) under test above the coils, with skin depth $\delta = 8.3$ mm distorts the magnetic field of the sensing coil, while the reference coil measures the ambient.

The change in eddy current is reflected as a voltage change across the sensor coil. By measuring the change in voltage, the magnitude of displacement can be estimated. Similar arrangements can also be used to detect rotational displacements [19].

Yet another method to detect the presence of a metal is by use of pulse induction (PI). In this method, a single coil is used as both the transmitter and the receiver coil. A very low resistance coil is connected across a voltage source for a short period of time and is abruptly disconnected using a switch. The abrupt change in the current through the coil creates a high intensity voltage spike of opposite polarity in the coil. This spike decays in an exponential fashion. When a metallic object is present in the field of the sensor the object stores a part of the energy in the reflected pulse. This decreases the decay rate of the spike. Thus, by measuring the rate of decay, the presence or absence of a metal can be determined.

Metals such as Nickel are sensitive to high frequencies, gold to mid frequencies, whereas metals like iron are sensitive to all frequency regions. The PI method can also be used to differentiate between metals by varying the frequency at which the coil switches between transmitter and receiver mode.

Magnetoresistive elements are often used to determine physical properties of systems. When a current-carrying ferromagnetic alloy is subjected to an external magnetic field, electrical resistance of the alloy changes. The change in the electrical resistance is a function of the angle formed between the internal magnetization vector $\vec{M}$, and the vector of the electrical current $\vec{I}$ flowing through it. Hence, when a strong magnetic field H is applied, the magnetoresistive element operates in saturation mode. In this mode, the current field strength has negligible effect, and hence the resistance is entirely determined by the direction of the magnetic field. This is useful in non-contact angular measurement applications [20].

4.2. Property Estimation

Determining the conductivity profile of a conductor is important for various industrial applications, such as quality assurance, coating processes, and surface treatment. The measurement made using a PI sensor can be further processed to derive the conductivity profile of the material. The conductivity of the material determines the eddy current in the material. The eddy current in the material influences the decay rate. Hence by measuring the decay rate, the conductivity of the material can be estimated.

Eddy current sensors, such as the ones shown in Figs. 12 and 13, can be used to determine conductivity σ, permeability μ, or thickness of the material. The skin depth δ over which the eddy current is large is given by:

$$\delta = \frac{1}{\sqrt{\pi f \mu \sigma}} \qquad (29)$$

where f is the frequency of excitation. Hence, by knowing any of the three variables, the fourth can be determined. The most common application of this sensor is to detect variation in the conductivity of the material. This is done by varying the excitation frequency, f, thus altering the depth δ at which the material is interrogated.

For layered material, the measured decay rate is a function of the properties of each layer. Since the number of measured quantities is less than that of the independent variables, the conductivity distribution cannot be directly calculated by analytical equations. The same holds true for determining the dielectric profile for multilayered materials. The measured transimpedance is a complicated function of the dielectric permittivity or magnetic permeability, the conductivity, and thickness of each layer.

The inversion of physical characteristics of layered media has been extensively studied [21]. The Gel'fand-Lecitan procedure is one of the well established methods to determine the conductivity profile. This procedure relates the reflection profile obtained from the PI sensor in the time domain with the characteristic profile through an integral equation. There are numerous methods to solve this integral equation, the most common of them being the differential operator technique. This technique provides an exact solution for the Butterworth case. Another widely used method is a numerical method that treats the Gel'fand-Lecitan leapfrogging in a space-time diagram. The characteristic profiles can also be obtained by adopting a step-by-step approach based on the electromagnetic wave integral equation in the time domain. However, for this method to perform satisfactorily, the front of the response has to be traced accurately.

For many sensors there exists no closed form analytical solution for the field distribution. Mathematical tools such as Fourier analysis, conformal mapping techniques (such as the Schwarz-Christoffel transformation), and finite difference and finite element analysis are helpful in solving boundary value problems. Each of these methods have their own merits and drawbacks. Fourier analysis is the simplest tool. However, it has an infinite term expansion of the series, and hence is not always practical. The Schwarz-Christoffel transformation is the most used method for two-dimensional analysis of Laplacian field distributions. This method, however has problems with convergence of the solution for nonsymmetrical problems. The most involved, but accurate, numerical methods to solve for the field distribution are the finite difference and finite element methods. These techniques are often used in two-dimensional as well as three-dimensional models.

4.3. Process Monitoring

To ensure consistent quality of a product, it is imperative to continually monitor the manufacturing process. The fringing field sensors, due to their non-invasive non-contact nature, are frequently used for this purpose.

4.3.1. Resin Transfer Molding

One of the typical applications of fringing field sensors is in monitoring for flow front position of fluids. In the control of Resin Transfer Molding (RTM) processes for the manufacture of thermoset composites [22, 23], it is difficult to fill the mold uniformly with the resin, without creating air-pockets, if the flow front is not continuously monitored. To enable this, fringing electric field sensors are embedded in the rigid mold along the expected flow lines. When the mold

is empty, the sensors measure the dielectric permittivity of the body of the mold, and that of the pre-form. Once, the resin starts to flow over the sensors, the effective permittivity as measured by the sensors increase. The greater the area of the sensor covered by the resin, the greater is the measured capacitance. This increase in effective permittivity can then be mapped onto the distance covered by the resin.

The increase in effective permittivity or measured capacitance can be used to obtain information on the flow. The first order differential of the distance–time curve provides information on the velocity of flow. Based on Darcy's law, the velocity of flow, along the pressure differential along the velocity vector, can be used to estimate the viscosity of the resin as

$$\mu = -\frac{k}{V_x}\frac{\partial P}{\partial x} \tag{30}$$

where V_x is the average speed of the resin along the x direction, k is the permeability of the porous medium, μ is the viscosity of the fluid and $\partial P/\partial x$ is the pressure gradient in the x direction.

4.3.2. Thermoset-Curing

Dielectric properties also change dramatically during the curing process of thermosetting resin matrix composite materials when the resin transforms from a monomeric liquid into a cross-linked insoluble solid material [24]. Thus, the same sensor used to measure the flow front of the resin, can also be used to monitor the curing process [25]. The curing process is often monitored by measuring the relaxation constants of the dielectric. Hence the sensor is excited at different frequencies to obtain the Cole–Cole plot [26], which plots the imaginary part of the complex dielectric constant versus the real part with frequency as a parameter, from which the information on the relaxation processes can be extracted. For Debye relaxation, given by (25)–(27), the Cole–Cole plot is a semi-circle. Deviations from a semicircle indicate other polarization phenomena such as electric double layer effects.

With the introduction of lower frequency measurements, the double layer effects become particularly important. The role of the double layer in both parallel plate measurements and microdielectrometry measurements were studied in [27]. A polarization model was developed to explain this phenomenon. An analytical treatment of the double-layer impedance based on the continuum-model simulations of [28] is presented in [29, 30].

4.3.3. Moisture Diffusion

Fundamental analysis of moisture diffusion processes is conducted in [31, 32]. In this investigation, the moisture diffusion coefficients are measured in thin polymer films through monitoring changes in permittivity. The dielectric properties are measured within the first 10 μm of the film thickness. The total film thickness is about 100 μm. By 1992, the frequency range of operation was extended over the range from 0.001 Hz to 100 kHz. The alternation of wet and dry environments allows measurement of diffusion coefficients for both absorption and desorption. Because of electrode polarization double layer effects, the reported measurement was

limited to the single frequency of 10 kHz. The dynamic analysis relies on the evidence available from the literature that the dielectric constant changes linearly with moisture content in polyimides [33] and epoxies [34]. A one-dimensional diffusion process is modeled with the traditional solution to Fick's law [35].

Moisture dynamics in a power transformer oil-paper environment were investigated using three dielectric sensors like that in Fig. 1 on a common substrate with three different wavelengths of 1, 2.5, and 5 mm. Such multi-wavelength sensors can measure distributions of material properties, in this case measuring moisture profiles in oil-free and oil-impregnated transformer pressboard as a function of time and measuring the moisture diffusion coefficient as a function of moisture and temperature [36–39].

GLOSSARY

Alternating current (AC)   Flowing charge carriers in a conductor or semiconductor which periodically reverse direction as a function of time.

Bias current or voltage   A current or voltage that is independent of output applied to an electronic device to facilitate proper operation by adjusting proper voltage, charge, or current conditions into the proper operating regime.

Charge density   The electric charge per unit area (surface charge density) or per unit volume (volume charge density) of an electrically charged body or a region of space.

Conformal mapping   A conformal mapping is a transformation that preserves local angles with a change of variables so that boundary shapes change to a simpler form allowing two-dimensional solutions to Laplace's equation in terms of the transformed variables.

Corner frequency   The cut-off frequency between the passband and stop-band where the signal attenuates by 3 dB.

Crosstalk   Electromagnetic interference between two or more wires.

Current density   The amount of current flowing through a unit cross-sectional area.

Dielectrometry   The study of lossy dielectric material properties.

Dielectric permittivity   A constant of proportionality between electric displacement field $\vec{D}$ and electric field $\vec{E}$; it is a measure of how much a material capacitance changes when a vacuum gap is replaced by media.

Dipoles   An electric or magnetic dipole pair of equal and opposite electric or magnetic charges separated by a small distance. A magnetic dipole can also be considered a current loop with small area.

Direct current (DC)   The unidirectional flow or movement of electric charge carriers, usually electrons in metals for which the intensity of the current can vary with time, but without change in polarity.

Double layer effect   Charge separation that occurs at the interface between oppositely charged ions in solution and an electrode forming two layers of charge separated by a small distance approximately given by the Debye length. The ions redistribute to balance the charge held by the electrode,

resulting in a potential drop confined to the double layer region in which this occurs; often a fixed charge layer on the wall and a mobile layer of counter charge in adjacent fluid.

Eddy currents   A current induced in a conductor in response to a changing magnetic field.

Electric field   The electric field is defined in terms of the electrostatic force per charge that would be exerted on a test charge placed in the field.

Electric scalar potential   Also known as voltage, it is a measure of the potential energy per unit charge.

Electrode   A collector or emitter of electric charge, usually an equipotential metal conductor.

Electroquasistatic   Based on low-frequency approximations to Maxwell's equations, it assumes that the electric field is irrotational.

Ferromagnetic   Characteristic of exhibiting spontaneous magnetism originating from the unpaired electron spin in a material.

Field lines   A set of lines drawn such that they are everywhere parallel to the direction of the field.

Filter   A circuit that passes or attenuates desired frequencies.

Fringing electric field sensor   A capacitive sensor that does not require two-sided access.

Ground   The zero reference level used to apply and measure voltages in a circuit.

Impedance   Opposition to the flow of current when a voltage is applied, equal to the ratio of voltage complex amplitude to current complex amplitude. It is a complex value composed of a real part representing lossy elements and an imaginary part of energy storage due to capacitive and inductive elements.

Inductance   A circuit element that stores magnetic energy.

Interdigital   A digitlike or fingerlike periodic pattern of electrodes or windings.

Leakage currents   Parasitic current flowing across regions in which no current should be flowing if the material properties are ideal.

Loss angle   The phase angle between the imaginary and real part of complex permittivity or complex magnetic permeability.

Loss factor   The tangent of the loss angle which represents the ratio of the imaginary to the real part of complex permittivity or complex magnetic permeability.

Magnetic field   The field that results from moving charges (currents) or a magnetized material.

Magnetic flux   The measure of the strength and direction of a magnetic field equal to the total magnetic field passing perpendicular through a surface area.

Magnetic permeability   The ability of a substance to acquire magnetization due to a magnetic field; equal to the ratio of $\vec{B}/\vec{H}$ in linear media.

Magnetoresistive   A material in which electrical resistance changes when subjected to a magnetic field.

Magnetoquasistatic   Based on approximations to Maxwell's equations, it assumes sufficiently low frequency

that displacement current density is negligible in Ampere's law.

Multiplexer   A device in which two or more input signals share one output node.

Mutual inductance   A measure of the flux through a circuit due to the current in another circuit.

Non-polar   Characterized by not having a separation of charge in an electric field such that no positive and negative poles are formed, as in oxygen.

Penetration depth   This term relates to how far an electric or magnetic field can penetrate into a given material under test.

Polar   Having a pair of equal and opposite charges that maintain a small separation, such as in water.

Polarization   In electrostatics, the contribution to the displacement field $\vec{D}$ due to the dipole separation of charges; equal to the number of electric dipoles per unit volume.

Quasistatic   When time rates of change are sufficiently slow that the governing equations are of similar form to time invariant conditions.

Self inductance   Gives the inductance related to magnetic flux due to current in the same conductor.

Sensor head   The sensor area where the sensing electrodes are located.

Signal conditioning   The process and equipment for converting the signal from the sensor to the correct level and frequency for an analog to digital converter.

Signal processing   The manipulation of data to enhance/extract the representations of physical or electrical phenomena.

Spatial wavelength   The spatial periodicity distance between the centerlines of adjacent electrode or winding fingers belonging to the same electrode or winding family.

Spectroscopy   The study of a material's property dependence upon frequency.

Transimpedance   From the term transfer impedance, it refers to the ratio between a voltage change at the output terminal due to a related change of current at the input terminal.

Virtual ground   A point in a circuit that acts as a ground level potential but does not have any physical connection to it.

Wavelength   The distance between successive peaks or troughs of a periodic wave.

REFERENCES

1. A. V. Mamishev, K. Sundara-Rajan, F. Yang, Y. Du, and M. Zahn, *Proceedings of the IEEE* 92(5), 808 (2004).
2. M. Zahn and H. A. Haus, *Journal of Electrostatics* 34(2–3), 109 (1995).
3. M. Zahn and H. A. Haus, *Journal of Electrostatics* 34(2–3), 109 (1995).
4. Y. Sheiretov, Ph.D. thesis, MIT, Department of Electrical Engineering and Computer Science, 2001.
5. N. Goldfine, D. Schlicker, Y. Sheiretov, A. Washabaugh, and V. Zilberstein, "ASME Turbo Expo, Land, Sea, & Air," New Orleans, LA, 2001.

6. J. Fischer, N. Goldfine, and V. Zilberstein, "49th Defense Working Group on NDT," Biloxi, Mississippi, 2000.

7. N. Goldfine, A. Washabaugh, V. Zilberstein, D. Schlicker, J. Fischer, T. Lovelett, T. Yentzer, and R. Pittman, "USAF ASIP Conference," San Antonio, TX, 2000.

8. T. Yentzer, V. Zilberstein, N. Goldfine, D. Schlicker, and D. Clark, "Fourth DoD/FAA/NASA Conference on Aging Aircraft," St. Louis, MO, 2000.

9. A. W. Kraszewski, "Microwave Aquametry." IEEE Press, 1996.

10. P. Debye, "Polar Molecules." Chemical Catalog Co., 1929.

11. J. R. MacDonald, "Impedance Spectroscopy: Emphasizing Solid Materials and Systems." Wiley, New York, 1987.

12. J. Fraden, "AIP Handbook of Modern Sensors: Physics, Design, and Applications." American Institute of Physics, 1993.

13. H. R. Taylor, "Data Acquisition for Sensor Systems." Chapman & Hall, 1997.

14. R. C. Franklin and F. I. Fuller, USA 4099118, 1978.

15. P. W. Kithil, U.S.A. 5,366,241 (9-22-1994).

16. P. W. Kithil, U.S.A. 5,602,734 (2-11-1997).

17. P. W. Kithil, U.S.A. 5,691,693 (9-25-1997).

18. C. H. Bruce, USA 5506506 (1996).

19. D. E. Johnson, USA 4868504 (1989).

20. L. Jansseune, B. Legrand, J. Voyant, and J. Yonnet, "Planar-Coil Displacement Sensors" (R. K. Jurgen, Ed.), 2nd Edition, pp. 153–157. Society of Automotive Engineers, Inc., 2003.

21. M. Wesser and A. Harmansa, "Novel Self-Monitoring Magnetoresistive Sensor System for Automotive Angular Measurement Applications" (R. K. Jurgen, Ed.), 2nd Edition, pp. 159–166. Society of Automotive Engineers, Inc., 2003.

22. I. Kay, "The Inverse Scattering Problem." New York Univ. Res. Rep., 1955.

23. A. A. Skordos, P. I. Karkanas, and I. K. Partridge, 11(1), 25 (2000).

24. M. Hegg, Master of Science in Electrical Engineering Thesis, University of Washington, Seattle, 2004.

25. J. S. Kim and D. G. Lee, B30(2), 159 (1996).

26. N. F. Sheppard, Jr., S. L. Garverick, D. R. Day, and S. D. Senturia, "Proceedings of the 26th SAMPE Symposium," 1981.

27. K. S. Cole and R. H. Cole, 9(4), 341 (1941).

28. D. R. Day, T. J. Lewis, H. L. Lee, and S. D. Senturia, 73 (1984).

29. M. C. Zaretsky, Ph.D. thesis, Department of Electrical Engineering and Computer Science, Massachusetts Institute of Technology, 1987.

30. P. A. von Guggenberg, "Conference on Electrical Insulation and Dielectric Phenomena," 1993.

31. N. F. Sheppard Jr., R. C. Tucker, and C. Wu, 65(9), 1998 (1993).

32. D. R. Day and D. D. Shepard, "Nondestructive Monitoring of Materials Properties Symposium," 1988.

33. D. R. Day, D. D. Shepard, and K. J. Craven, 32(8), 524 (1992).

34. D. D. Denton, D. R. Day, D. F. Priore, S. D. Senturia, E. S. Anolick, and D. Scheider, 14(2), 119 (1985).

35. P. D. Aldrich, S. K. Thurow, M. J. M.Kennon, and M. E. Lyssy, 28(13), 2289 (1987).

36. J. Crank, "The Mathematics of Diffusion," Clarendon Press, 1956.

37. Y. Du, A. V. Mamishev, B. C. Lesieutre, M. Zahn, and S. Lindgren, 1 (1999).

38. A. V. Mamishev, Y. Du, J. H. Bau, B. C. Lesieutre, and M. Zahn, *IEEE Transactions on Dielectrics and Electrical Insulation* 8(5), 785 (2001).

39. Y. Du, Department of Electrical Engineering and Computer Science, Massachusetts Institute of Technology, 1999.

40. Y. Du, B. C. Lesieutre, and M. Zahn, "EPRI," Palo Alto, CA, 2000.